Hydrogen Storage

Enhancing H$_2$ Uptake by "Close-Packing" Alignment of Open Copper Sites in Metal–Organic Frameworks**

*Xi-Sen Wang, Shengqian Ma, Paul M. Forster, Daqiang Yuan, Juergen Eckert, Joseph J. López, Brandon J. Murphy, John B. Parise, and Hong-Cai Zhou**

Recently, porous metal-organic frameworks (MOFs)[1] have been studied as a promising class of materials to reach the U.S. Department of Energy (DOE) targets[2] for vehicular hydrogen storage.[3] Continuing effort has been devoted to the enhancement of hydrogen affinity[4] in MOFs, thus increasing hydrogen uptake. Strategies reported lately include introducing framework interpenetration[3e,j] and constructing pores to fit the size of the hydrogen molecule.[3b,c] Particular attention has been paid to the creation of open metal sites,[4a,d,e,5a,b] which has proven to be an effective way of strengthening the MOF–H$_2$ interaction.

Herein, our strategy to enhance H$_2$ uptake is to strengthen the MOF–H$_2$ interaction by increasing the number of nearest neighboring open metal sites of each H$_2$-hosting void in a 3D framework and to align the open metal sites so that they can interact directly with the guests (H$_2$ molecules) inside the void.

In the close-packing of spheres, with structures such as cubic close-packing (ccp) or hexagonal close-packing (hcp), each sphere has a maximum of 12 nearest neighbors. Connecting the 12 neighbors gives rise to a cuboctahedron for ccp or an anticuboctahedron for hcp. In the case of hydrogen-storing MOFs, if the central sphere is removed and the void used to host H$_2$, then the MOF–H$_2$ interaction can be strengthened by placing open metal sites at the 12 corners of the cuboctahedron or anticuboctahedron (Figure 1a).
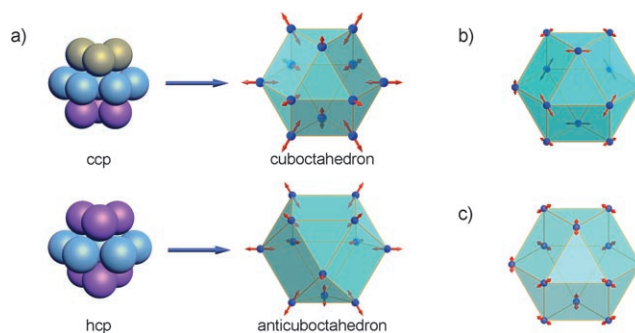

Figure 1. a) Two common types of close-packing of spheres and their corresponding polyhedra; red arrows demonstrate the ideal placement of open coordination sites of paddlewheel dimetal units; b) One cuboctahedron drawn using atomic coordinates retrieved from the crystal data of HKUST-1.[8] Red arrows show the orientations of the open metal-coordination sites; c) Cuboctahedron drawn using atomic coordinates from the crystal data of MOF-505 with an emblematic NbO-type topology.[3f] Red arrows demonstrate the out-of-alignment open metal-coordination sites.

By using isophthalate and a dimetal paddlewheel structural motif, a cuboctahedral cage or an anticuboctahedral cage can be prepared.[6] If the isophthalate motif is extended at the 5 position using another moiety that contains one or more carboxylate groups, the polyhedron can be extended into a cuboctahedral or anticuboctahedral framework, which should have high hydrogen uptake. Although quite a few MOFs with appreciable hydrogen uptake have been intuitively constructed this way,[3i,j,7] the open metal sites in these MOFs are often misaligned[7] because of the geometric constraints of the ligands, which prevent the further enhancement of the MOF–H$_2$ interaction (Figure 1b and c).

A possible design for an "ideal" ligand for the construction of a MOF based on cuboctahedral cages with aligned open metal sites is to keep the two isophthalate moieties to ensure the formation of the cuboctahedral cages but link the two using a bent bridge to prevent the formation of an NbO-type structure. A ligand designed using such a strategy is 5,5′-methylene-di-isophthalate[9] (mdip, Figure 2). Herein we report the synthesis of two Cu–mdip MOFs that are polymorphs of each other: a MOF consisting of cuboctahedra with all the open metal sites aligned, PCN-12 (PCN represents porous coordination network), and PCN-12′, in which the open metal sites are out of alignment, as the basis for comparison (Figure 3).

The reason that polymorphism arises in Cu-mdip MOFs is due to the two extreme conformations of mdip: a form with C_s point group symmetry, in which the two benzene rings of mdip are perpendicular to each other (Figure 2a); and a C_{2v} form

[*] Dr. X.-S. Wang, Dr. S. Ma, Dr. D. Yuan, J. J. López, B. J. Murphy, Prof. Dr. H.-C. Zhou
Department of Chemistry
Texas A & M University
PO Box 30012, College Station, TX 77842-3012 (USA)
Fax: (+1) 513-529-0452
E-mail: zhou@mail.chem.tamu.edu

Prof. Dr. P. M. Forster, J. B. Parise
Mineral Physics Institute, Stony Brook University
Stony Brook, NY 11794 (USA)

Prof. Dr. J. Eckert
Materials Research Laboratory
University of California, Santa Barbara, CA 93106-5621 (USA)

Supporting information (including experimental data) for this article is available on the WWW under http://dx.doi.org/10.1002/anie.200802087.
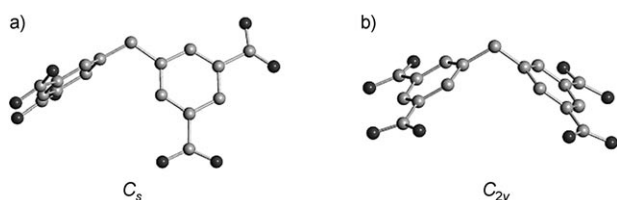
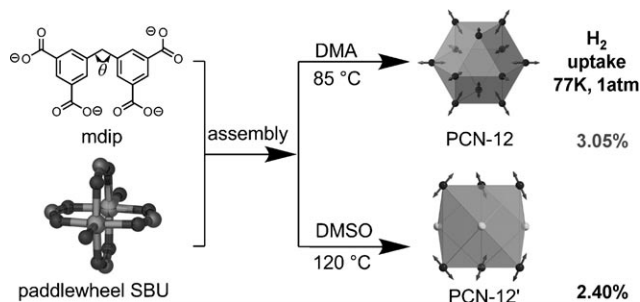**Figure 2.** Two extreme conformations of 5,5′-methylene diisophthalate (mdip, gray C, black O).

Figure 3. The synthesis, open metal site alignment, and hydrogen uptake of the two MOF polymorphs: PCN-12 and PCN-12′.

Figure 4. a) A cuboctahedral cage in PCN-12; b) a rhombicuboctahedron in PCN-12. In both, the open Cu sites point toward the center of the cage, as illustrated in Figure 1 a.

that can be generated by symmetry with one-fourth of the ligand (Figure 2b). PCN-12 exhibits a record-high hydrogen uptake of 3.05 wt% at 77 K and 1 atm (for a MOF), in contrast to an uptake of 2.40 wt% for PCN-12′ under the same conditions. The remarkable difference in hydrogen uptake for the two MOFs reflects the dissimilar open metal site alignments in the two polymorphs (Figure 3).

Crystals of PCN-12 were grown under solvothermal reaction conditions from a mixture of $Cu(NO_3)_2 \cdot 2.5 H_2O$ and $H_4(mdip)$ in dimethylacetamide (DMA) at 85 °C. The products were isolated as dark-blue block-shaped crystals with the formula $[Cu_6(C_s\text{-mdip})_2(C_{2v}\text{-mdip})(H_2O)_6] \cdot 3 DMA \cdot 6 H_2O$ (yield: 85%), which was determined by a combination of X-ray crystallography, elemental analysis, and thermogravimetric analysis (TGA) data (full experimental details are found in the Supporting Information).

Single-crystal X-ray analysis using microcrystal diffraction at the Advanced Photon Source reveals that PCN-12 crystallizes in the tetragonal space group $P4/mmm$.[10] It adopts a dicopper paddlewheel motif as its secondary building unit (SBU, Figure 3); the copper atoms become coordinatively unsaturated upon removal of the axial aqua ligand.

The paddlewheel SBU occupies the 12 vertices of a cuboctahedron (Figure 4a) while 24 isophthalate motifs span all 24 edges. The square faces are 11.2 Å in dimension (Cu–Cu distance along the diagonal), and the triangular faces are 7.9 Å in dimension (Cu–Cu distance along the edge). As expected, at the 12 corners of the cuboctahedron, there are 12 open copper-coordination sites pointing toward the center of the cage. Each square face is connected to another square face of a neighboring cuboctahedron through four mdip bridges (see Supporting Information, Figure S1). Every cuboctahedron connects to six others in three orthogonal directions to form a 3D net.
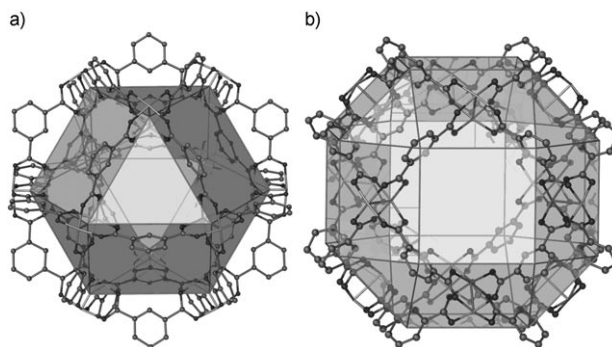
Whereas intuition would place the vertices of the net at the paddlewheel, a recognizable continuous network becomes apparent if instead the centers of the phenyl rings are used as nodes. This network, designated 3.4^4, consists of rhombicuboctahedra (Figure 4b) and cubes.[11]

The overall idealized symmetry of the net would have been $Pm\bar{3}m$. However, the mdip ligands along the a and b axes hold point-group symmetry of C_s but those along the c axis possess C_{2v} symmetry. The conformational difference of mdip ligands lowers the overall symmetry from cubic to tetragonal.

In C_{2v}-mdip, the phenyl rings face each other and form an angle, θ, of 110.6° at the C atom of the methylene group (Figure 2b) while the dihedral angle is almost identical (110.3°) to θ. These angles are also similar to the ideal bond angles (109.5°) surrounding a tetrahedral C atom. Conversely, the C_s-mdip has a dihedral angle of 89.6° with $\theta = 116.2°$. The deviation from 109.5° is due to the repulsion of the two phenyl rings (Figure 2a). It can be deduced that, at higher temperature, the C_s-mdip may be converted to the C_{2v} form, leading to the formation of a polymorph of PCN-12, containing only C_{2v}-mdip ligands. Indeed, such a polymorph, PCN-12′, has been obtained by a reaction between $Cu(NO_3)_2 \cdot 2.5 H_2O$ and H_4mdip in dimethylsulfoxide (DMSO) at 120 °C (full experimental details are in the Supporting Information).

Single-crystal X-ray analysis reveals that PCN-12′,[12] $[Cu_2(C_{2v}\text{-mdip})(H_2O)_2] \cdot 3 DMSO$, crystallizes in the space group $P6_3/mmc$. Every mdip ligand in PCN-12′ has C_{2v} symmetry. Each of the six paddlewheels connects three mdip ligands in a trigonal-prismatic fashion with paddlewheel units occupying all corners of the "prism" (Figure 5a) and the three mdip ligands residing on the three sides. Evidently, the open metal coordination sites (Figure 5b, red arrows) point away from the cavity of the polyhedron. If the methylene groups of the mdip ligands are counted as vertices (Figure 5b, yellow spheres) together with the six paddlewheels, the structural unit can be viewed as a tricapped-trigonal-prism (TTP) with 9 vertices, 14 faces, and 24 edges. Every three TTPs are further connected by mdip ligands to three more TTPs in the next layer, the TTPs being related by the 6_3 axes (Figure 5c). The projection of the structure on [001] has the symmetry of a Kagome pattern (Figure 5c).[13]
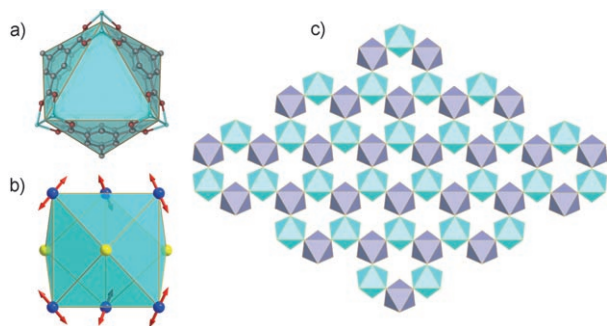
Figure 5. A tricapped trigonal prismatic cage viewed a) from the top and b) from one side; the red arrows demonstrate the orientations of the open metal-coordination sites and the yellow spheres represent methylene groups of the three mdip ligands; c) PCN-12′ viewed from the [001] direction.

The structures of PCN-12 and PCN-12′ are quite different from those of the MOFs assembled from other diisophthalates, all of which have linear ligands and NbO-type structures.[3f,8] Viewed from the space-filling diagrams, both PCN-12 and PCN-12′ are porous (see Supporting Information, Figures S2 and S3). After the removal of guest solvates and axial aqua ligands, the total solvent-accessible volume of PCN-12′ is 67.4%, slightly lower than that of PCN-12 (70.2%). These values were calculated using the PLANTON routine.[14] The calculated density of structures after removal of solvent is 0.762 and 0.851 $g cm^{-3}$ for PCN-12 and PCN-12′, respectively.

The nitrogen adsorption isotherms, as shown in Figure 6a, reveal that both PCN-12 and PCN-12′ exhibit typical type-I adsorption behavior. The Langmuir surface area, BET surface area, and pore volume of PCN-12 are 2425 $m^2 g^{-1}$,
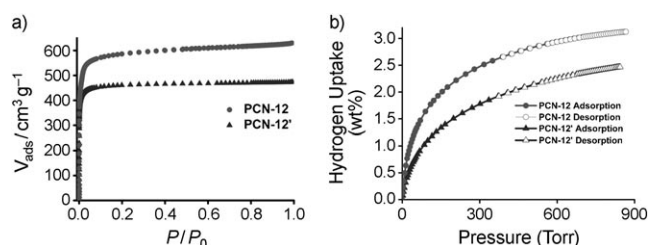

Figure 6. Gas adsorption isotherms for PCN-12 and PCN-12′: a) N_2 and b) H_2.

1943 $m^2 g^{-1}$, and 0.94 $mL g^{-1}$, respectively, whereas those for PCN-12′ are 1962 $m^2 g^{-1}$, 1577 $m^2 g^{-1}$, and 0.73 $mL g^{-1}$, respectively. Studies have shown repeatedly that there is no simple correlation between surface area and hydrogen uptake of a MOF at 77 K and 1 atm.[4e]

The hydrogen adsorption isotherm of PCN-12′ (Figure 6b) shows a 2.40 wt% $(20.4 g L)^{-1}$ hydrogen uptake at 77 K and 1 atm, comparable to those of other MOFs containing cuboctahedral cages (Table 1). However, PCN-12 exhibits an exceedingly high hydrogen uptake of 3.05 wt% $(23.2 g L^{-1})$ under the same conditions.

This high hydrogen uptake of PCN-12, compared to PCN-12′, can be ascribed to both the formation of cuboctahedral cages and the alignment of open metal sites within each cage.

However, when compared to other MOFs containing cuboctahedral cages (Table 1), the enhancement of hydrogen uptake can probably be attributed to the unique alignment

Table 1: Hydrogen uptake [wt%] of microporous MOFs with cuboctahedral cages at 77 K and 1 bar measured volumetrically unless otherwise designated.

Material	Uptake	Material	Uptake
PCN-12	3.05	PCN-10[7b]	2.34
MOF-505[7a]	2.59[a]	Mn-BTT[5a,b]	2.25
PCN-11[7b]	2.55	Cu_2(qptc)[7a]	2.24[a]
HKUST-1[3g]	2.54	PCN-6[3i,j]	1.90
Cu_2(tptc)[7a]	2.52[a]	PCN-9[4a]	1.53
Cu-BTT[5b]	2.42	PCN-6′[3j]	1.35
PCN-12′	2.40		

[a] denotes gravimetric measurements.

of the open copper sites in PCN-12, strengthening the H_2–framework interaction. To our knowledge, PCN-12 possesses the highest hydrogen uptake reported for a MOF at 1 bar and 77 K.

To check the reproducibility of the high H_2 uptake for PCN-12, five additional measurements, using five different PCN-12 samples with mass ranging from 40 mg to 250 mg, were performed. The average hydrogen uptake of the six measurements is 3.05 wt% with a standard deviation of 0.035 wt% (see Supporting Information, Figure S4).

The INS (inelastic neutron scattering) spectrum of the hindered rotor transitions for six H_2 molecules per formula unit, $[Cu_6(C_s\text{-mdip})_2(C_{2v}\text{-mdip})]$, adsorbed in activated PCN-12 (Figure 7) is characterized by a very intense, structured band near 8 meV, with relatively little intensity in the region between 11 meV and 14.5 meV. The latter region has been shown in previous work[15a] to be associated with dihydrogen adsorbed on or near the organic linker, whereas the transitions in the range of the strong peak are attributed to H_2 molecules at the open Cu^{II} sites. The loading used in this experiment (one H_2 per open copper-coordination site, or 1 wt%) would be sufficient to fill all the available Cu sites if these were indeed strongly preferred over other binding sites. Hence we can readily associate the broad band in the range of 7–10 meV with 0–1 rotational tunneling transitions of H_2
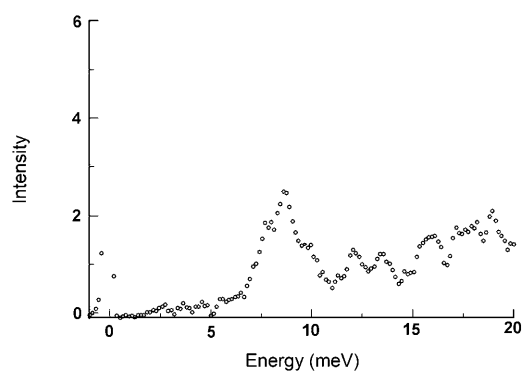

Figure 7. The inelastic neutron scattering spectrum of PCN-12.

interacting with open Cu sites. The two principal components of this band at 7.7 meV and 8.6 meV occur at 0–1 transition energies appreciably lower than that of the paddlewheel SBU Cu site in HKUST-1 (9 meV),[15b] thereby indicating a much stronger interaction of H_2 with the Cu sites in PCN-12. A qualitative indication of this trend is provided by the Cu–OH_2 distances determined from the removable aqua-ligand at Cu. In PCN-12 such bond lengths range from 2.116 Å to 2.172 Å with an average of 2.138 Å, whereas in HKUST-1, the Cu–OH_2 distance was found to be 2.165 Å.[8] If we assume that the Cu···H_2 distances in the two compounds compare in a similar way, the lower rotational tunneling transition frequencies (higher barriers to rotation) in PCN-12 can be qualitatively understood. More details on the analysis and interpretation of the rotational INS spectra of H_2 in PCN-12, and their relevance to the exceptionally strong interaction of H_2 with this host will be presented elsewhere.

As polymorphs of each other, PCN-12 and PCN-12′ have not only the same formula after solvate removal but also the same atom-to-atom connectivity. However, the gravimetric hydrogen uptake of PCN-12 is 27% higher than that of PCN12′ at 77 K and 1 bar. The reason behind these remarkable improvements can mainly be attributed to the "close-packing" strategy, namely, the formation of cuboctahedral cages and the unique alignment of open metal sites in each cuboctahedral cage in PCN-12. This strategy may have general implications in the search for a practical adsorptive hydrogen-storage material for fuel-cell-driven cars.

[1] a) S. Kitagawa, R. Kitaura, S. i. Noro, *Angew. Chem.* **2004**, *116*, 2388–2430; *Angew. Chem. Int. Ed.* **2004**, *43*, 2334–2375; b) N. W. Ockwig, O. Delgado-Friedrichs, M. O'Keeffe, O. M. Yaghi, *Acc. Chem. Res.* **2005**, *38*, 176–182; c) X. S. Wang, S. Ma, D. Sun, S. Parkin, H. C. Zhou, *J. Am. Chem. Soc.* **2006**, *128*, 16474–16475; d) S. Ma, D. Sun, X. S. Wang, H. C. Zhou, *Angew. Chem.* **2007**, *119*, 2510–2514; *Angew. Chem. Int. Ed.* **2007**, *46*, 2458–2462; e) S. Ma, D. Sun, J. M. Simmons, C. D. Collier, D. Yuan, H. C. Zhou, *J. Am. Chem. Soc.* **2008**, *130*, 1012–1016.

[2] DOE Office of Energy Efficiency and Renewable Energy Hydrogen, Fuel Cells & Infrastructure Technologies Program Multi-Year Research, Development and Demonstration Plan, available at: http://www.eere.energy.gov/hydrogenandfuelcells/mypp.

[3] a) J. L. C. Rowsell, A. R. Millward, K. S. Park, O. M. Yaghi, *J. Am. Chem. Soc.* **2004**, *126*, 5666–5667; b) L. Pan, M. B. Sander, X. Huang, J. Li, M. R. Smith, Jr., E. W. Bittner, B. C. Bockrath, J. K. Johnson, *J. Am. Chem. Soc.* **2004**, *126*, 1308–1309; c) B. Kesanli, Y. Cui, R. Smith Milton, W. Bittner Edward, C. Bockrath Bradley, W. Lin, *Angew. Chem.* **2005**, *117*, 74–77; *Angew. Chem. Int. Ed.* **2005**, *44*, 72–75; d) D. Sun, Y. Ke, T. M. Mattox, A. O. Betty, H. C. Zhou, *Chem. Commun.* **2005**, 5447–5449; e) J. L. C. Rowsell, O. M. Yaghi, *Angew. Chem.* **2005**, *117*, 4748–4758; *Angew. Chem. Int. Ed.* **2005**, *44*, 4670–4679; f) B. Chen, N. W. Ockwig, A. R. Millward, D. S. Contreras, O. M. Yaghi, *Angew. Chem.* **2005**, *117*, 4823–4827; *Angew. Chem. Int. Ed.* **2005**, *44*, 4745–4749; g) J. L. C. Rowsell, O. M. Yaghi, *J. Am. Chem. Soc.* **2006**, *128*, 1304–1315; h) B. Chen, S. Ma, F. Zapata, E. B. Lobkovsky, J. Yang, *Inorg. Chem.* **2006**, *45*, 5718–5720; i) D. Sun, S. Ma, Y. Ke, D. J. Collins, H. C. Zhou, *J. Am. Chem. Soc.* **2006**, *128*, 3896–3897; j) S. Ma, D. Sun, M. W. Ambrogio, J. A. Fillinger, S. Parkin, H. C. Zhou, *J. Am. Chem. Soc.* **2007**, *129*, 1858–1859; k) H. Chun, D. N. Dybtsev, H. Kim, K. Kim, *Chem. Eur. J.* **2005**, *11*, 3521–3529.

[4] a) S. Ma, H.-C. Zhou, *J. Am. Chem. Soc.* **2006**, *128*, 11734–11735; b) Y. Li, R. T. Yang, *J. Am. Chem. Soc.* **2006**, *128*, 726–727; c) Y. Li, R. T. Yang, *J. Am. Chem. Soc.* **2006**, *128*, 8136–8137; d) P. M. Forster, J. Eckert, B. D. Heiken, J. B. Parise, J. W. Yoon, S. H. Jhung, J. S. Chang, A. K. Cheetham, *J. Am. Chem. Soc.* **2006**, *128*, 16846–16850; e) D. J. Collins, H. C. Zhou, *J. Mater. Chem.* **2007**, *17*, 3154–3160.

[5] a) M. Dincă, A. Dailly, Y. Liu, C. M. Brown, D. A. Neumann, J. R. Long, *J. Am. Chem. Soc.* **2006**, *128*, 16876–16883; b) M. Dincă, W. S. Han, Y. Liu, A. Dailly, C. M. Brown, J. R. Long, *Angew. Chem.* **2007**, *119*, 1441–1444; *Angew. Chem. Int. Ed.* **2007**, *46*, 1419–1422.

[6] a) Y. Ke, D. J. Collins, H. C. Zhou, *Inorg. Chem.* **2005**, *44*, 4154–4156; b) G. J. McManus, Z. Wang, M. J. Zaworotko, *Cryst. Growth Des.* **2004**, *4*, 11–13; c) M. Eddaoudi, J. Kim, J. B. Wachter, H. K. Chae, M. O'Keeffe, O. M. Yaghi, *J. Am. Chem. Soc.* **2001**, *123*, 4368–4369; d) B. Moulton, J. Lu, A. Mondal, M. J. Zaworotko, *Chem. Commun.* **2001**, 863–864; e) F. Nouar, J. F. Eubank, T. Bousquet, L. Wojtas, M. J. Zaworotko, M. Eddaoudi, *J. Am. Chem. Soc.* **2008**, *130*, 1833–1835.

[7] a) X. Lin, J. Jia, X. Zhao, K. M. Thomas, A. J. Blake, G. S. Walker, N. R. Champness, P. Hubberstey, M. Schröder, *Angew. Chem.* **2006**, *118*, 7518–7524; *Angew. Chem. Int. Ed.* **2006**, *45*, 7358–7364; b) X. S. Wang, S. Ma, K. Rauch, J. M. Simmons, D. Yuan, X. Wang, T. Yildirim, W. C. Cole, J. J. López, A. de Meijere, H. C. Zhou, *Chem. Mater.*, DOI: 10.1021/cm800403d.

[8] S. S.-Y. Chui, S. M. F. Lo, J. P. H. Charmant, A. G. Orpen, I. D. Williams, *Science* **1999**, *283*, 1148–1150.

[9] J. K. Leblanc, D. B. Sharp, J. C. Murray, *J. Org. Chem.* **1961**, *26*, 4731–4733.

[10] Crystal data for PCN-12: $C_{51}H_{30}Cu_6O_{30}$, M_r = 1510.04, turquoise block, tetragonal, space group *P4/mmm*, $a = b = 32.868(4)$, $c = 22.627(4)$ Å, $\alpha = \beta = \gamma = 90°$, $V = 24444(6)$ Å^3, $Z = 8$, $\rho_{calcd} = 0.814$ g cm^{-3}, R_1 for $I > 2\sigma$ (I): 0.085, wR_2 for all data: 0.254, GOF = 1.05. CCDC 662918, CCDC 662919 contains the supplementary crystallographic data for this paper. These data can be obtained free of charge from The Cambridge Crystallographic Data Centre at www.ccdc.cam.ac.uk/data_request/cif.

[11] M. O'Keeffe, B. G. Hyde, *Crystal Structures: I. Patterns and Symmetry*, Mineralogical Society of America, Washington, **1996**.

[12] Crystal data for PCN-12′: $C_{17}H_{10}Cu_2O_{10}$, M_r = 501.33, turquoise block, hexagonal, space group *P6₃/mmc*, $a = b = 18.07(2)$, $c = 19.34(2)$ Å, $\alpha = \beta = 90°$, $\gamma = 120°$, $V = 5469(10)$ Å^3, $Z = 6$, $\rho_{calcd} = 0.910$ g cm^{-3}, R_1 for $I > 2\sigma$ (I): 0.076, wR_2 for all data: 0.224, GOF = 1.108.[10]

[13] I. Syôzi, *Prog. Theor. Phys.* **1951**, *6*, 306–308.

[14] A. L. Spek, *J. Appl. Crystallogr.* **2003**, *36*, 7–13.

[15] a) J. L. C. Rowsell, J. Eckert, O. M. Yaghi, *J. Am. Chem. Soc.* **2005**, *127*, 14904–14910; b) Y. Liu, C. M. Brown, D. A. Neumann, V. K. Peterson, C. J. Kepert, *J. Alloys Compd.* **2007**, *446–447*, 385–388.